Journal of Geophysical Research - Planets

Supporting Information for

Formation of Tridymite and Evidence for a Hydrothermal History at Gale Crater, Mars

A. S. Yen[1], R. V. Morris[2], D. W. Ming[2], S. P. Schwenzer[3], B. Sutter[2], D. T. Vaniman[4], A. H. Treiman[5], R. Gellert[6], C. N. Achilles[7], J. A. Berger[2], D. F. Blake[8], N. I. Boyd[6], T. F. Bristow[8], S. Chipera[9], B. C. Clark[10], P. I. Craig[4], R. T. Downs[11], H. B. Franz[7], T. Gabriel[12], A. C. McAdam[7], S. M. Morrison[13], C. D. O'Connell-Cooper[14], E. B. Rampe[2], M. E. Schmidt[15], L. M. Thompson[14], S. J. VanBommel[16]

[1]Jet Propulsion Laboratory, California Institute of Technology, Pasadena, California 91109
[2]NASA, Johnson Space Center, Houston, Texas 77058
[3]The Open University, Milton Keynes, UK
[4]Planetary Science Institute, Tucson, Arizona 85719
[5]Lunar and Planetary Institute, Houston, Texas 77058
[6]University of Guelph, Guelph, Ontario, Canada
[7]NASA, Goddard Space Flight Center, Greenbelt, Maryland 20771
[8]NASA, Ames Research Center, Moffett Field, California 94035
[9]Chesapeake Energy Corporation, Oklahoma City, Oklahoma 73118
[10]Space Science Institute, Boulder, Colorado 80301
[11]University of Arizona, Tucson, Arizona 85721
[12]Arizona State University, Tempe, Arizona 85281
[13]Carnegie Institution, Washington, D. C. 20015
[14]University of New Brunswick, Fredericton, New Brunswick, Canada
[15]Brock University, St. Catharines, Ontario, Canada
[16]Washington University in St. Louis, St. Louis, Missouri 63130

Contents of this file

Introduction

Supporting figures and captions plus a summary of the data used in this manuscript are included in this Supporting Information file.

Supporting Figures

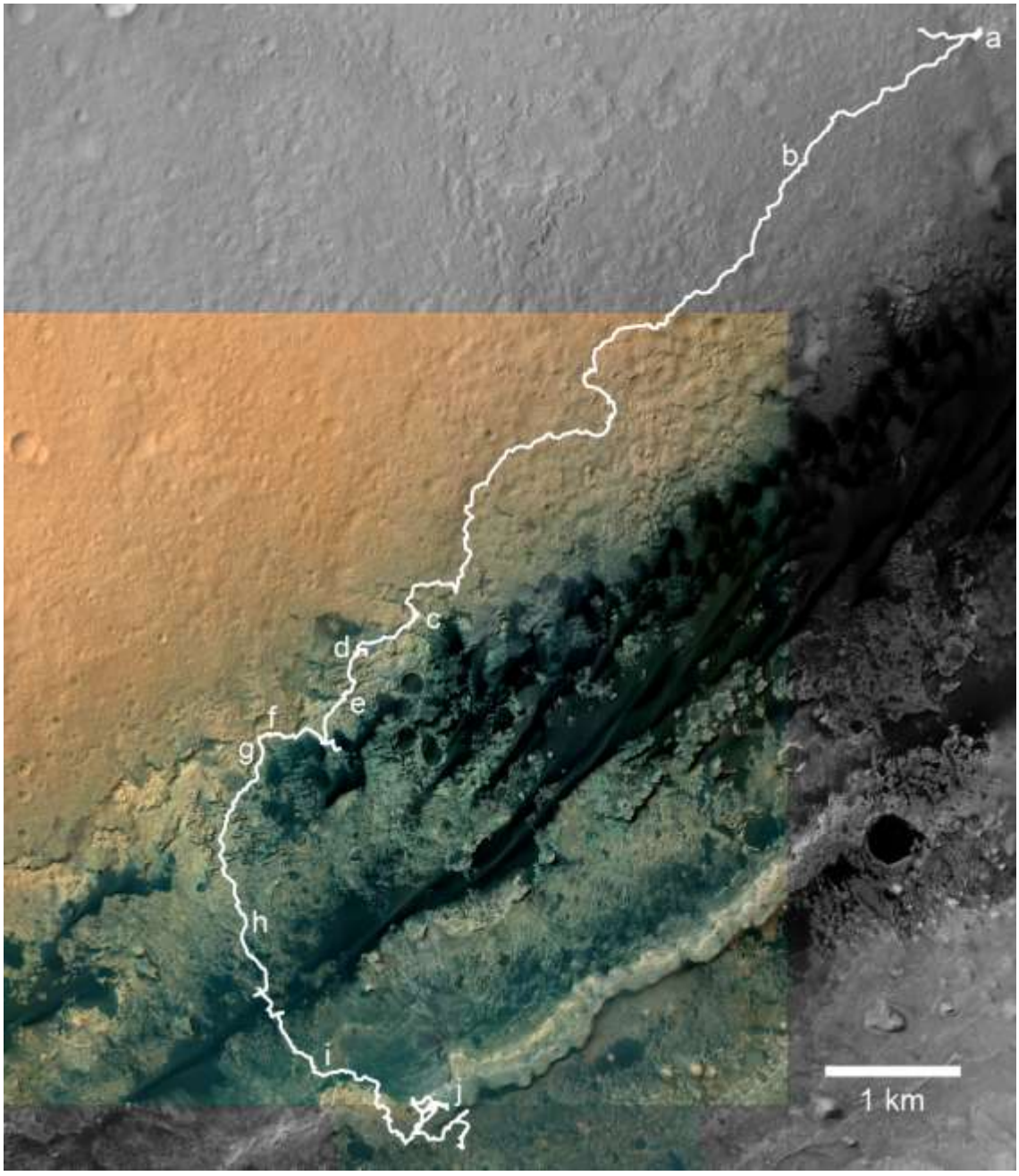

Figure S1. Curiosity rover traverse map highlighting regions with possible hydrothermal histories discussed in the manuscript: (a) Cumberland (sol 279) and John Klein (sol 182) drill holes, (b) silica-rich alteration halo (sol 392, Fig. 2g, [Williams et al., 2014]), (c) Murray formation at Pahrump Hills, including Telegraph Peak drill sample (sol 909), and Garden City veins (sol 930, Fig. 2d), (d) high-silica Murray, including Buckskin drill sample (sol 1060, Fig. 2c), (e) first complete analysis of alteration halo in Stimson sandstone (two drill samples): Big Sky (sol 1119) and Greenhorn (sol 1137), (f) second complete analysis of alteration halo in Stimson sandstone (two drill samples): Okoruso (sol 1332) and Lubango (sol 1320, Fig. 2a), (g) Oudam drill sample (Murray formation, sol 1361), (h) Thrumcap alteration halo (sol 1504, Fig. 2e), (i) example of nodular Se-rich sample (Berry Cove, sol 1714, Fig. 2f), (j) Vera Rubin Ridge.

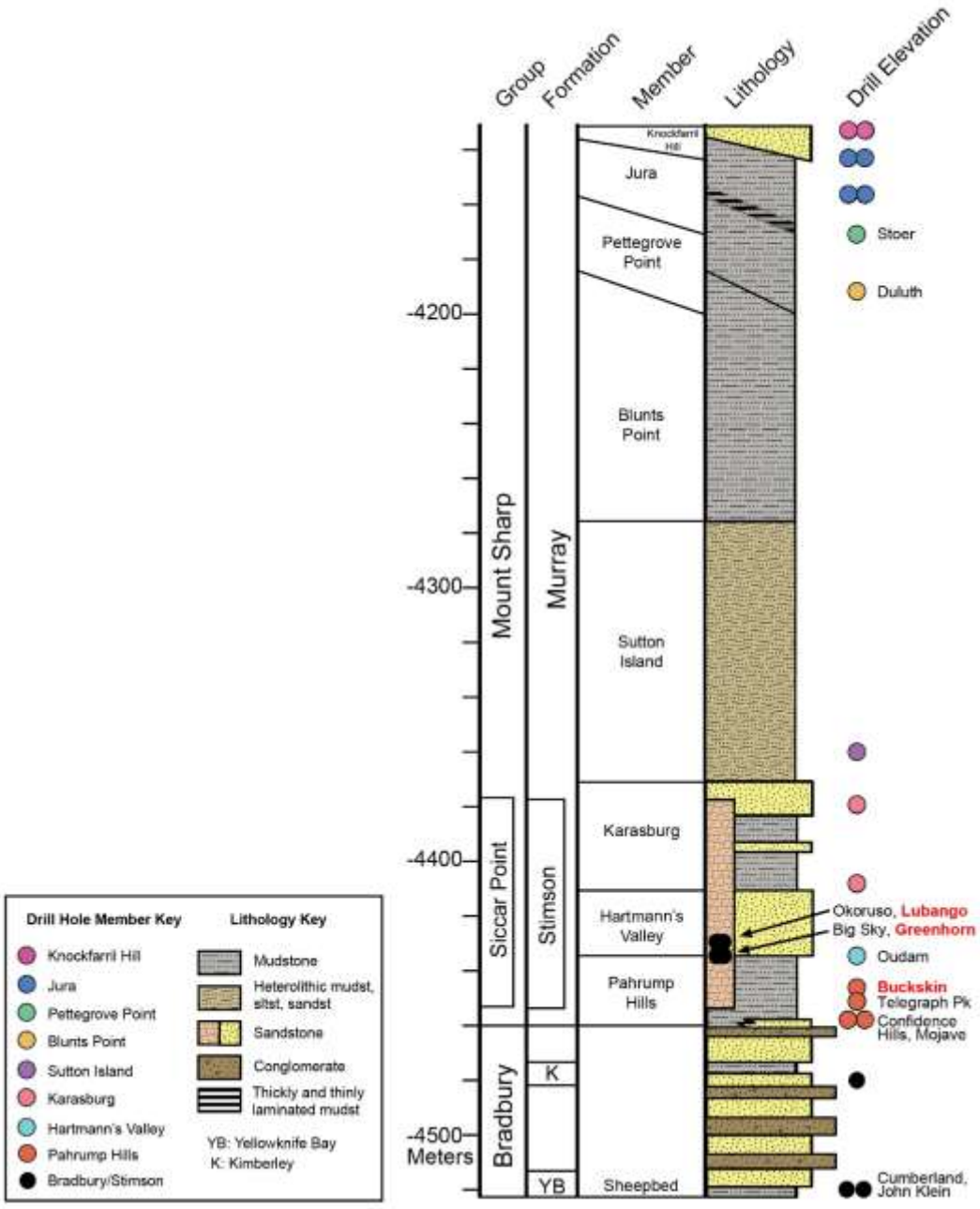

Figure S2. Stratigraphic column of Gale crater (product of the *MSL Sedimentology and Stratigraphy Working Group*). The Murray formation from the base of the Pahrump Hills through the Jura member covers ~320 meters of elevation. Drill holes discussed in the text are labeled by name, and the silica-rich samples proposed as hydrothermal in origin are highlighted in red: Buckskin is in the Murray formation, and Lubango and Greenhorn are in the Stimson formation.

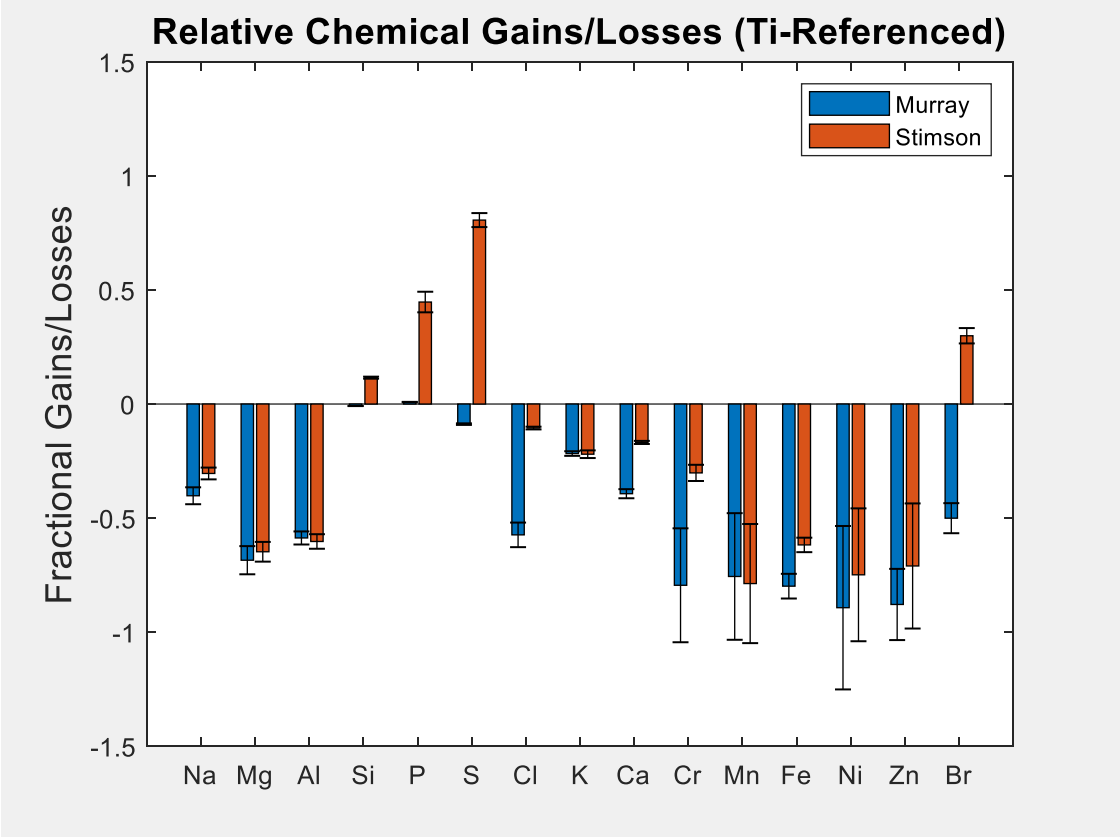

Figure S3. Titanium-referenced gains and losses [Nesbitt, 1979] of silicified Murray and Stimson formation samples relative to representative parent material. Murray formation samples show significant Ti-referenced losses in all elements except Si, P, and S, consistent with acidic leaching. Similar depletions of major elements are observed in silicified Stimson formation alteration halos, and gains in P, S, and Br may represent secondary precipitation.

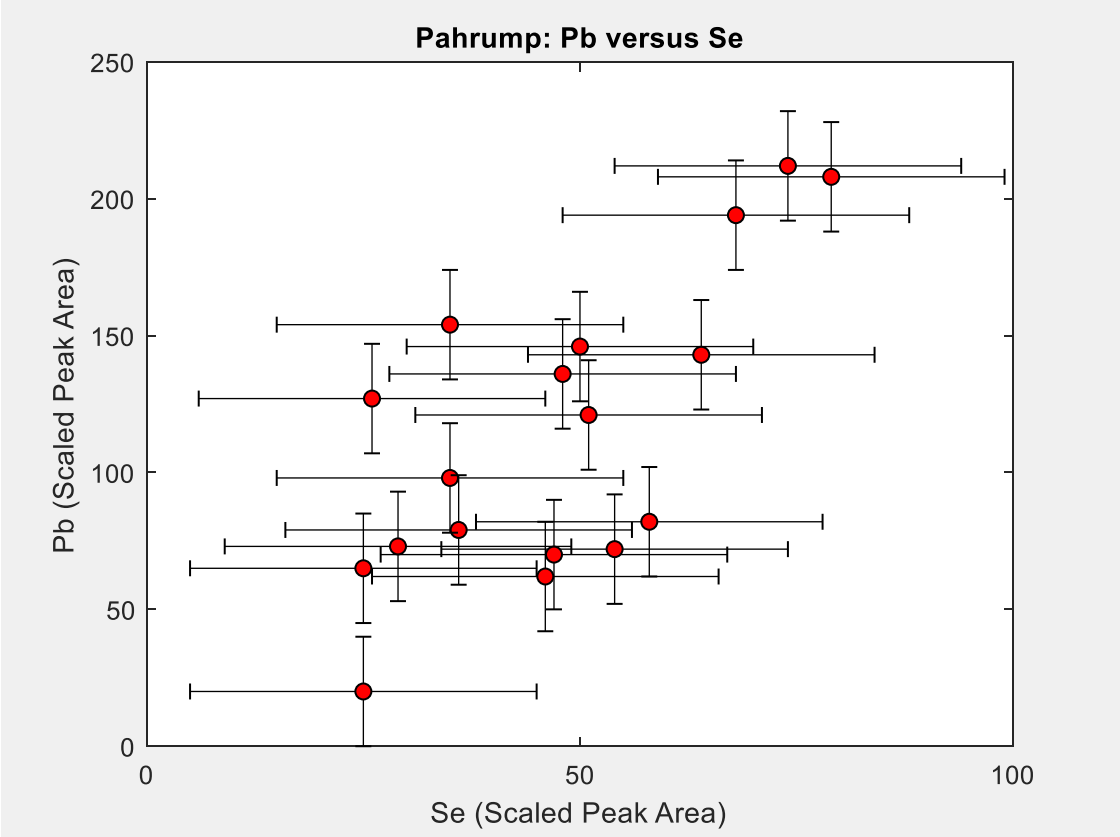

Figure S4. APXS measurements for lead and selenium in the Pahrump member of the Murray formation. This apparent correlation ($R^2 = 0.5$) is consistent with mobility in a single fluid, possibly at elevated temperatures. Outside of the Pahrump region, Se values are not as uniformly elevated and not consistently associated with Pb, suggesting that multiple fluid processes were responsible for the mobility of these trace elements within Gale crater.

Figure S5. Target "Lamoose," an eroded, finely-laminated, silica-enriched (73 wt% SiO_2) sample amidst layered, rubbly regolith (portion of mcam04555, sol 1039). The preservation of layering has been used to argue against in-situ silicification and to support detrital accumulations of silicic material. However, preservation of layering is observed in diagenetic silica-rich rocks (e.g. Fig. 2b), so layering does not necessarily imply that the initial sediments were derived from silicic source material. This sample was not drilled for mineralogical analyses, and it is not known if it contains tridymite.

Supporting Data

APXS data used in the manuscript are available in tabulated form from the Planetary Data System (DOI for the MSL APXS RDR dataset: 10.17189/1518757): https://pds-geosciences.wustl.edu/msl/msl-m-apxs-4_5-rdr-v1/mslapx_1xxx/extras/

Figure 1: The individual APXS analyses contributing to each member (Fig. S2) of the Murray formation are listed below by the 3- or 4-digit sol number and the analysis start time. APXS targets not used in Figure 1 are those with any of the following characteristics: >15 wt% SO_3, >60 wt% SiO_2, clear diagenetic features in the APXS field of view, and one or more elemental concentrations more than 4 standard deviations from the mean. The numerical values for Figure 1 are provided in Table SI.

Figure 3a: Drill samples are represented by APXS analyses of mini-start hole drill cuttings (from the preparatory drill hole) when available, as they are unsieved and represent the bulk composition of the sample. In contrast to the drill cuttings from the main hole used to acquire sample for CheMin and SAM, the mini-drill hole is analyzed within one sol of the drilling, minimizing the aeolian erosion of the sample. Due to arm positioning constraints, the cuttings from the main drill hole cannot typically be analyzed until >5 sols after drilling. Specific samples used for Figure 3a: Lubango (1325M02:58:21: full drill cuttings, 5 sols after drilling; mini-start hole not used), Okoruso (1337M23:14:47: full drill cuttings, 5 sols after drilling; mini-start hole not used), Greenhorn (1134M22:27:33: mini-start hole, same sol as drilling), Big Sky (1116M22:01:46: mini-start hole, same sol as drilling), Buckskin (1059M19:41:01: mini-start hole, same sol as drilling), Confidence Hills (759M10:40:48: mini-start hole, 2 sols after drilling).

Figures 3b and S3: The Stimson (typical and high-Si) and Murray (high-Si) samples used for Figures 3b and S3 are listed below. The high-Si Murray ratios are computed against the composition of the Pahrump member, as this is where the high-Si Murray samples are located. The numerical values used in the ratio and tau plots are provided in Table SI.

Pahrump member of Murray formation:

755M20:10:54	759M10:40:48	762M22:14:12	767M18:22:56	782M00:08:14	805M10:56:47	805M11:24:48	805M19:00:20	806M23:03:02	808M19:05:14
808M22:26:53	809M19:06:36	809M21:37:10	810M19:35:12	813M18:50:53	813M21:16:14	814M18:48:57	815M18:55:04	815M20:44:24	819M23:38:45
820M23:18:48	824M18:16:21	824M19:13:59	828M18:24:45	830M19:01:49	831M19:14:18	833M22:39:35	853M18:26:33	854M19:10:02	867M18:59:55
871M19:32:37	880M21:54:01	881M22:43:00	884M18:44:17	888M23:51:45	889M19:03:25	894M21:32:37	905M19:37:37	937M00:02:42	954M19:32:36

Hartmann's Valley member of Murray formation:

989M19:24:48	1109M20:54:25	1157M18:47:20	1157M21:18:15	1166M19:16:24	1191M23:17:41	1245M16:38:02	1245M21:03:03	1251M21:46:31	1253M20:04:25
1259M17:19:40	1259M22:38:40	1266M17:12:21	1266M22:38:58	1273M16:09:01	1273M19:28:17	1275M20:32:24	1355M17:05:57	1355M19:36:38	1358M17:40:28
1358M22:39:30	1364M22:21:19	1366M18:28:00	1368M20:41:09	1375M20:35:20	1376M10:47:23	1380M19:52:25	1380M20:34:16	1386M10:54:47	1403M18:57:30
1405M10:49:41									

Karasburg member of Murray formation:

1416M19:45:10	1417M01:44:10	1418M18:25:45	1418M19:09:07	1419M19:34:28	1426M22:17:31	1436M22:38:14	1444M18:32:50	1444M22:11:56	1457M18:58:48
1457M19:40:41	1459M20:50:39	1466M22:07:03							

Sutton Island member of Murray formation:

1474M19:48:09	1474M20:33:18	1477M22:34:29	1480M11:01:44	1484M18:42:39	1484M21:10:38	1491M18:50:58	1491M22:08:24	1493M23:21:39	1494M18:55:00
1494M19:31:33	1494M20:45:14	1496M22:09:25	1497M18:42:58	1504M18:35:02	1511M20:16:36	1512M03:35:58	1524M19:48:39	1525M22:35:52	1531M19:04:16
1531M22:17:37	1533M19:10:44	1552M19:15:43	1552M21:42:29	1569M22:02:56	1572M22:25:57	1576M10:58:27	1577M10:50:35	1581M22:28:44	1584M10:39:30
1586M19:13:35	1586M23:30:25	1589M10:55:08	1589M11:24:59	1591M10:55:57	1591M11:25:47	1593M19:13:10	1593M22:30:36	1596M11:05:51	1598M11:00:33
1600M19:59:18	1606M18:25:26	1609M21:23:11	1614M18:52:48	1614M20:35:55	1614M21:15:14	1614M22:23:53	1630M10:57:44	1632M10:54:23	1634M19:17:20
1634M20:57:57	1634M23:05:53	1640M20:27:27	1641M03:36:27	1644M22:27:59	1661M20:41:50	1662M02:32:05	1668M20:07:20	1668M21:46:20	1671M11:13:04
1677M11:00:34	1681M19:52:25	1681M20:13:30	1681M20:34:36	1681M20:55:40	1681M21:55:34				

Blunts Point member of Murray formation

1692M18:44:45	1692M22:23:05	1695M18:41:56	1698M11:43:53	1700M10:54:53	1714M22:32:59	1715M18:46:49	1715M21:05:52	1719M10:57:06	1721M11:37:57
1725M20:29:46	1725M22:19:37	1729M22:44:58	1736M20:08:05	1736M21:59:54	1744M18:35:49	1744M22:23:52	1753M11:06:12	1781M11:20:56	1784M00:05:26
1786M11:04:06	1788M10:49:10	1795M11:00:35	1796M10:57:55	1802M10:55:04	1806M18:13:28	2049M18:46:14	2050M00:42:07	2055M18:20:24	2080M19:49:25
2080M23:09:19	2082M02:48:57	2090M21:57:20							

Pettegrove Point member of Murray formation:

1809M10:56:49	1811M19:28:19	1811M23:31:35	1814M10:58:24	1816M20:27:39	1818M15:24:49	1818M18:54:07	1818M23:27:37	1821M19:15:23	1821M23:02:00
1824M19:23:36	1824M23:31:49	1829M10:51:50	1830M10:51:50	1834M11:46:54	1836M19:10:19	1836M23:23:42	1838M19:12:47	1838M22:06:51	1845M22:34:30
1853M02:15:29	1863M19:11:35	1863M21:30:38	1865M17:48:21	1865M20:25:47	1865M20:51:38	1865M22:45:29	1868M19:43:34	1870M19:50:16	1870M21:40:07
2000M18:17:40	2001M18:02:21	2001M20:06:38	2005M18:24:31	2005M22:16:49	2008M18:47:33	2008M21:41:04	2013M20:43:25	2014M10:53:19	2029M20:45:01
2032M11:05:12	2038M19:09:28	2042M18:37:47	2042M22:18:03	2100M22:27:08	2101M19:31:09	2101M21:30:36	2104M10:43:34	2109M22:17:09	2113M18:37:30
2113M22:04:23	2117M18:24:58	2121M18:47:34	2122M01:47:44	2124M18:28:17	2124M22:18:53	2127M19:05:36	2127M22:26:46	2131M18:17:29	2131M20:05:26
2131M20:47:47	2134M18:29:17	2134M23:14:13	2154M19:42:56	2154M22:23:16	2155M22:45:49				

Jura member of Murray formation:

1875M19:09:24	1875M22:04:28	1879M19:22:32	1879M22:57:13	1885M17:22:59	1885M22:00:32	1889M10:50:02	1892M18:23:17	1893M00:32:59	1895M18:19:42
1897M17:42:48	1897M20:05:52	1904M19:02:41	1904M22:04:52	1906M19:52:29	1907M01:50:23	1911M21:01:17	1921M16:58:52	1921M17:20:54	1921M17:41:32
1921M18:00:47	1921M21:40:05	1922M18:00:20	1925M22:08:42	1927M21:51:53	1929M21:45:25	1931M22:58:54	1934M18:53:35	1934M22:23:49	1940M17:11:28
1940M17:41:58	1940M21:40:42	1943M23:11:24	1945M21:47:53	1947M19:11:51	1947M23:24:26	1954M17:52:59	1954M20:52:16	1960M02:21:49	1963M19:16:37
1963M22:26:37	1966M19:14:39	1966M21:57:16	1972M19:40:13	1972M20:39:28	1975M20:38:39	1978M19:08:50	1979M18:58:14	1980M01:17:41	1984M18:45:49
1988M17:45:34	1988M20:11:25	1991M10:52:09	1993M11:39:13	1995M19:04:55	1995M20:49:59	2160M18:53:52	2165M18:11:24	2165M19:56:54	2165M22:16:04
2168M19:18:39	2168M23:24:44	2217M23:11:45	2220M18:46:47	2220M22:12:18	2223M19:06:08	2223M22:38:07	2245M19:22:02	2245M21:58:04	2247M22:29:30
2254M18:27:13	2255M01:05:19	2258M18:43:46	2258M22:02:58	2288M19:24:44	2289M02:34:21	2295M20:58:15	2299M11:06:00	2300M10:57:41	2301M20:42:24
2301M22:11:09									

High-silica Murray formation:

999M19:33:53	1041M19:17:36	1057M20:03:34	1057M20:47:47	1059M19:41:01	1064M23:17:29	1065M20:04:36	1089M20:32:34	1092M02:31:50	1110M01:37:12

Typical Stimson formation:

1092M21:34:28	1097M20:03:36	1114M19:06:03	1114M20:09:35	1116M22:01:46	1123M23:29:24	1124M20:02:33	1126M21:35:28	1132M22:26:14	1150M17:51:25
1150M22:18:47	1151M00:45:51	1277M16:34:15	1277M18:58:38	1278M01:51:47	1288M00:59:58	1294M01:51:52	1300M19:48:03	1330M17:49:14	1330M22:03:31
1337M23:14:47	1339M22:39:41	1341M17:32:30	1341M22:28:48	1348M18:18:31	1348M22:10:28	1351M18:41:30	1359M19:47:39		

High-silica Stimson formation:

1032M20:12:55	1091M20:30:52	1092M22:23:49	1130M21:24:11	1134M22:27:33	1142M23:23:15	1143M16:27:56	1143M22:13:58	1202M19:03:21	1202M20:45:41
1300M16:53:05	1313M23:57:31	1318M16:18:32	1318M17:46:45	1318M19:32:41	1319M18:28:50	1319M23:12:21	1325M02:58:21	1326M19:08:59	

Table SIa: Summary compositions for Murray and Stimson formations

		Na_2O	MgO	Al_2O_3	SiO_2	P_2O_5	SO_3	Cl	K_2O	CaO	TiO_2	Cr_2O_3	MnO	FeO_T	Ni	Zn	Br
Murray	Pahrump	2.77	5.24	10.97	50.28	1.19	5.49	0.70	0.75	4.62	1.09	0.36	0.33	15.83	0.075	0.162	0.021
	Hartmann's Valley	2.55	6.03	9.10	49.21	0.83	6.46	1.01	0.92	4.61	1.02	0.30	0.22	17.44	0.080	0.098	0.022
	Karasburg	2.30	5.18	8.60	46.54	1.00	7.60	1.17	0.81	5.22	1.04	0.30	0.15	19.80	0.097	0.091	0.033
	Sutton Island	2.38	5.91	8.59	46.37	1.05	7.30	1.39	0.81	4.48	1.04	0.32	0.22	19.78	0.085	0.113	0.037
	Blunts Point	2.30	5.97	8.39	45.25	1.12	6.98	1.14	0.83	4.58	1.06	0.31	0.29	21.37	0.085	0.169	0.036
	Pettegrove Point	2.58	5.58	8.94	46.69	0.92	6.51	1.40	0.92	4.56	1.04	0.32	0.24	19.98	0.089	0.107	0.015
	Jura	2.60	5.48	9.50	48.96	0.81	7.16	1.35	0.94	4.54	0.98	0.30	0.16	16.91	0.091	0.093	0.010
	High-silica	2.14	2.49	5.64	69.31	1.46	6.71	0.53	0.93	3.53	1.53	0.10	0.09	5.32	0.013	0.023	0.019
	Pahrump to Jura	2.53	5.65	9.20	47.71	0.97	6.79	1.23	0.87	4.58	1.03	0.32	0.23	18.58	0.086	0.116	0.022
Stimson	High-silica	2.31	3.50	4.49	59.03	1.45	11.20	1.24	0.39	6.46	1.10	0.35	0.09	8.20	0.013	0.011	0.035
	Typical	2.82	8.73	9.88	43.71	0.85	5.03	1.17	0.42	6.48	0.92	0.42	0.38	19.07	0.046	0.032	0.023

Table SIb: Standard deviations of summary compositions

		Na_2O	MgO	Al_2O_3	SiO_2	P_2O_5	SO_3	Cl	K_2O	CaO	TiO_2	Cr_2O_3	MnO	FeO_T	Ni	Zn	Br
Murray	Pahrump	0.20	1.08	1.07	2.81	0.18	1.59	0.34	0.12	1.11	0.07	0.05	0.07	2.22	0.024	0.044	0.024
	Hartmann's Valley	0.17	1.08	0.70	3.14	0.25	1.91	0.43	0.16	0.53	0.09	0.04	0.06	1.05	0.021	0.031	0.014
	Karasburg	0.18	0.52	0.30	1.41	0.20	1.64	0.44	0.06	0.98	0.03	0.02	0.05	1.07	0.009	0.010	0.026
	Sutton Island	0.19	0.99	0.56	3.66	0.31	3.27	0.46	0.13	1.84	0.08	0.04	0.13	2.39	0.017	0.049	0.030
	Blunts Point	0.17	1.38	0.44	3.35	0.13	3.20	0.53	0.15	1.90	0.08	0.04	0.14	2.12	0.019	0.040	0.024
	Pettegrove Point	0.17	0.73	0.41	2.27	0.15	1.69	0.65	0.11	1.17	0.05	0.03	0.09	1.65	0.011	0.028	0.013
	Jura	0.14	0.70	0.49	2.67	0.12	2.17	0.30	0.15	1.06	0.09	0.03	0.08	1.83	0.012	0.028	0.006
	High-silica	0.32	1.52	1.10	4.07	0.37	1.65	0.24	0.14	0.79	0.11	0.05	0.04	1.85	0.005	0.011	0.025
	Pahrump to Jura	0.22	0.97	0.97	3.34	0.24	2.45	0.52	0.15	1.35	0.08	0.04	0.11	2.63	0.017	0.045	0.023
Stimson	High-silica	0.27	1.54	1.41	3.94	0.41	2.02	0.74	0.09	1.41	0.14	0.08	0.03	3.09	0.007	0.004	0.016
	Typical	0.20	0.77	1.35	1.24	0.08	1.95	0.36	0.06	0.52	0.05	0.05	0.04	1.63	0.007	0.006	0.013